ECOLOGY LETTERS

Ecology Letters, (2015) **18**: 1311–1320 doi: 10.1111/ele.12525

LETTER

Water availability predicts forest canopy height at the global scale

Tamir Klein,[1]*† Christophe Randin,[1,2†] and Christian Körner[1]

[1]Institute of Botany University of Basel Schönbeinstrasse 6, Basel, 4056, Switzerland [2]Department of Ecology & Evolution University of Lausanne, Switzerland

**Correspondence: E-mail: tamir.klein@unibas.ch*

†These authors contributed equally to this work.

Abstract

The tendency of trees to grow taller with increasing water availability is common knowledge. Yet a robust, universal relationship between the spatial distribution of water availability and forest canopy height (H) is lacking. Here, we created a global water availability map by calculating an annual budget as the difference between precipitation (P) and potential evapotranspiration (PET) at a 1-km spatial resolution, and in turn correlated it with a global H map of the same resolution. Across forested areas over the globe, H_{mean} increased with P-PET, roughly: H_{mean} (m) = 19.3 + 0.077*(P-PET). Maximum forest canopy height also increased gradually from ~ 5 to ~ 50 m, saturating at ~ 45 m for P-PET > 500 mm. Forests were far from their maximum height potential in cold, boreal regions and in disturbed areas. The strong association between forest height and P-PET provides a useful tool when studying future forest dynamics under climate change, and in quantifying anthropogenic forest disturbance.

Keywords

Evapotranspiration, forest suppression, hydraulic constraints, range limits, tree height.

Ecology Letters *(2015)* ***18****: 1311–1320*

INTRODUCTION

A balance between tree structural strength and wind shearing forces sets an upper limit to tree height. But aside from these biomechanical constraints, it is counter-gravitational water transport that is considered the primary limit to tree height. In transpiring trees, the hydrostatic pressure is accompanied by hydrodynamic frictional resistances, also scaling with path length. With increasing height, the difficulty in hydrating leaves increases: leaves at treetops struggle to maintain turgor and have lower water potential (Ψ_{leaf}) than leaves at lower position in the canopy (Koch *et al*. 2004). Evidently, among factors affecting Ψ_{leaf} (solute concentration, xylem tension, matrix effects, etc.), only the height-related gravitational component exerts a constant effect, equal to −0.1 MPa per 10 m increase in tree height.

The decline in Ψ_{leaf} with increased height is a common pattern across all trees, but can vary among species due to differences in stomatal regulation and xylem architecture. Ψ_{leaf} decline was observed in twigs of redwoods (*Sequoia sempervirens*, among the tallest trees on earth) in the very humid temperate coastal forest of northern California, USA (Koch *et al*. 2004). In late summer, Ψ_{leaf} was reported to decrease from −1.2 MPa at 40 m to −1.9 MPa at 90 m, an evidence of increasing hydraulic limitation (Friend 1993; Ryan & Yoder 1997; Givnish *et al*. 2014). The critical biological action of this hydraulic limitation on tree height can be twofold: reduced stomatal conductance, and thus, reduced CO_2 uptake (C-limitation) or direct impact of turgor loss on tissue formation (growth limitation). Several studies, motivated by the question of the theoretical maximum tree height, have proposed a direct hydraulic limitation (Koch *et al*. 2004; Niklas & Spatz 2004; Pennisi 2005; Domec *et al*. 2008; Sala & Hoch 2009). Xylem cavitation risk can explain limitations in conifer height, as the pit aperture diameter of tracheids decreases steadily with height, thereby diminishing the water transport across the pits (Domec *et al*. 2008). From an ecological perspective, water input (mostly as rainfall) was shown to govern global plant height distributions (Moles *et al*. 2009; although not tested exclusively for trees). In their study of maximum plant height data from 7048 plant species x site combinations, precipitation during the wettest month was the best explanatory determinant of global plant height patterns among environmental variables. Precipitation was also the first component of a predictive global forest canopy height model, which was applied successfully at the continental scale over USA (Choi *et al*. 2013; Shi *et al*. 2013).

Recent years have seen the application of advanced remote sensing techniques in ecology (e.g. airborne LiDAR and satellite laser altimetry). This facilitated global maps of forest canopy height on the one hand (Lefsky 2010; Simard *et al*. 2011), and water availability patterns on the other (Zomer *et al*. 2006, 2008). Here, we take advantage of these global datasets and relate, at a 1-km spatial resolution, forest canopy height to a proxy of water availability (the difference between annual precipitation and potential evapotranspiration, P-PET). Furthermore, the relationship between forest canopy height and P-PET was used to test the extent to which forest height could be locally predicted from P-PET. We hypothesized that: (1) both the mean and maximum forest canopy height should increase with increasing P-PET up to an upper threshold, and (2) the predictability of tree height from P-PET should be generally high and decrease at higher latitudes and elevations, presumably due to temperature limitations.

MATERIAL AND METHODS

Approach

An equation was calibrated with maximum and mean forest canopy height (H) as response variables, P-PET as a predicting

variable and a Gaussian error distribution. Here, we used the global map of canopy height at a 0.00833-degree (30 arc-seconds and ~ 1 km) spatial resolution (http://lidarradar.jpl.nasa.gov/; last accessed: December 17, 2013) developed by Simard *et al*. (2011) and based on 2005 data from the Geoscience Laser Altimeter System (GLAS) aboard ICESat (Ice, Cloud and land Elevation Satellite). Simard *et al*. (2011) complemented the GLAS-derived canopy height values at a mean coverage of 121 data points degree^{-2} by modelling down to 1-km pixel resolution, using forest type, tree cover, elevation and climatology maps. The resulting map was validated with *in situ* canopy heights measured at 66 Fluxnet sites (RMSE = 6.1 m, $r^2 = 0.5$; or, RMSE = 4.4, $r^2 = 0.7$ without seven outliers). Evidently, annual precipitation was one of seven ancillary variables used in the smoothing process of the map. But since (1) evapotranspiration (potential or actual) was not used in the production of the final map, (2) the independent contribution and the importance of precipitation alone in the model used for smoothing was most likely low with six other explanatory variables, (3) the model was used mostly to estimate canopy height values for areas not covered by GLAS waveforms and, overall, (4) the core of the dataset was based on direct satellite observations, the level of inescapable circularity in our analysis was likely very low to negligible.

P-PET was the best integrative proxy for more complex hydrological processes available with the same extents and resolution as the map of canopy height and was calculated from global climate layers and remote sensing data (Hijmans *et al*. 2005; Zomer *et al*. 2006, 2008; Trabucco & Zomer 2010) further filtered to include forest land cover exclusively (Arino *et al*. 2008). Data sources and spatial resolutions for the variables used in the analysis are summarized in Table 1.

Table 1 Data sources and spatial resolutions for the variables used in the analysis

Variable	Dataset	Year	Resolution (Decimal deg)	References
Forest canopy height	Forest canopy height	2005	0.00833	Simard *et al*. (2011)
Monthly mean P	WorldClim	1950–2000	0.00833	Hijmans *et al*. (2005)
Monthly mean PET	CGIAR-CSI	1950–2000	0.00833	Zomer *et al*. (2008)
Monthly mean T, TD	WorldClim	1950–2000	0.00833	Hijmans *et al*. (2005)
Yearly AET	FAO	1961–1990	0.00833	
Forest land cover	GlobeCover	2009	0.00277	Arino *et al*. (2008)
Human footprint	SEDAC	2000	0.00833	Sanderson *et al*. (2002)

P, precipitation; PET, potential evapotranspiration; T, temperature; TD, daily temperature range; AET, actual evapotranspiration; ESA, European Space Agency.

Water availability index

We generated a global map of the difference between annual precipitation and potential evapotranspiration (P-PET). This layer was computed as the sum of the monthly difference between actual water inputs from precipitation and the atmospheric forcing from potential evapotranspiration (PET). Maps of monthly P (mm/month) were obtained from WorldClim (Hijmans *et al*. 2005) and monthly average PET (mm/month; Hargreaves method) from the CGIAR-CSI consortium (Zomer *et al*. 2008; http://www.cgiar-csi.org/data; last accessed December 17 2013) at a spatial resolution of 0.00833 degree (30 arc-seconds) and for the 1950–2000 reference period. Note that under conditions of increased atmospheric demand to water vapour, PET increases and typically diverges from actual evapotranspiration to such extent that P-PET can decrease to as low as −2000 mm year^{-1}. The Hargreaves PET was tested against four other techniques (Holland, Thornthwaite, Modified Hargreaves and Penman-Monteith, used by the UN Food and Agriculture Organization, FAO), when generating the CGIAR-CSI dataset. It was validated with observations in Africa (January: Mean difference = 22.3 mm SD = 16.1; July: Mean difference = 20.0 mm SD = 19.3) and South America (January: Mean difference = 38.2 mm SD = 19.2; July: Mean difference = 27.2 mm SD = 14.0). The Hargreaves PET overestimates the FAO Penman-Monteith PET by up to 101 mm year^{-1} at PET < 942 mm year^{-1}, and underestimates it at higher values (e.g. by 113 mm year^{-1} at PET = 2000 mm year^{-1}), but generally they correlate well ($r^2 = 0.99$; Xu & Singh 2002). It has recently been shown that proxies such as P-PET were outperformed by soil water balance indices when representing available water for trees (Piedallu *et al*. 2013). However, P-PET is so far the best proxy available for global analysis since comprehensive global soil databases and the corresponding soil water holding capacities are not yet available at the global scale.

Spatial analysis

The global map of remotely sensed forest canopy height was filtered to remove land cover categories that would have biased the analysis. First, we only considered canopy height >2 m. Second, we used the global land cover geo-dataset GlobeCover 2009 from the European Space Agency (Arino *et al*. 2008; http://due.esrin.esa.int/globcover/; version 2.3, last accessed December 17, 2013) to extract forested areas at the global scale at a 0.00277-degree (~ 300 m) spatial resolution. The categories considered in our analysis are listed in Table S1. This spatial layer was resampled to match the spatial resolution of the climate layers and the map of canopy height. Corresponding values of P-PET were extracted for each filtered pixel of canopy height and the mean and maximum values of canopy height were then extracted for each 1-mm increment of P-PET with R custom code (R Development Core Team, 2011).

A second filtration step was performed to produce the mean forest canopy height in Fig. 1c using the global human footprint map as an additional layer, by filtering all data to human footprint < 5% (http://sedac.ciesin.columbia.edu/data/set/wildareas-v2-human-footprint-geographical/maps). As reported in Sanderson *et al*. (2002), human footprint values are produced through an overlay of a number of global data layers that represent the location of various factors presumed

to exert an influence on ecosystems: human population distribution, urban areas, roads, navigable rivers and various agricultural land uses. The combined influence of these factors yields the human influence index. The Human Influence Index, in turn, is normalized by global biomes to create the human footprint values, ranging from 1 to 100. Here, we used the version of the human footprint map of the year 2000 at a resolution of 0.00833 degree.

Maximum forest canopy heights were still lower than reported maximum canopy heights in undisturbed, protected areas (Koch *et al*. 2004; Domec *et al*. 2008), hinting at an overarching effect of anthropogenic perturbation (Toniato & de Oliveira-Filho 2004). Unfortunately, the size of such plots was smaller than the 1-km spatial resolution in this study. To correct for this anthropogenic perturbation, we applied two approaches: (1) Mean forest height was recalculated, using the global human footprint map (Sanderson *et al*. 2002) as an additional layer, by filtering all data to a human footprint < 5%; and (2) Using a statistical approach, by smoothing the maximum H around the highest value within P-PET moving windows of 250 mm, yielding an additional equation, termed here absolute maximum. Different parameterizations were tested for the three equations of H as function of P-PET (absolute maximum, maximum and mean), from a simple linear relationship with polynomial function of order 4. Equations with the best fit were the ones with polynomial functions of order 4 for P-PET. In search for a simple, elegant saturation curve, a Michaelis–Menten type model was additionally fitted to the observed maximum H by P-PET. For this purpose, all P-PET values were made positive by adding 2000; the overall maximum was determined as the observed 69 m; and the P-PET value at half the overall maximum (34.5 m) was calculated as the mean of 40 observed values at H = 34 m and 67 observed values at H = 35 m, yielding a normalized P-PET of 852 mm.

Additional parameters of water availability

Obviously, P-PET is an over-simplification of more complex hydrological and plant processes, which jointly determine the water availability of forest stands. At best, P-PET should approximate the balance between water inputs (as precipitation and infiltration) and water losses through evapotranspiration, i.e. the soil water content integrated over a a month or a year. We additionally calculated water availability from the

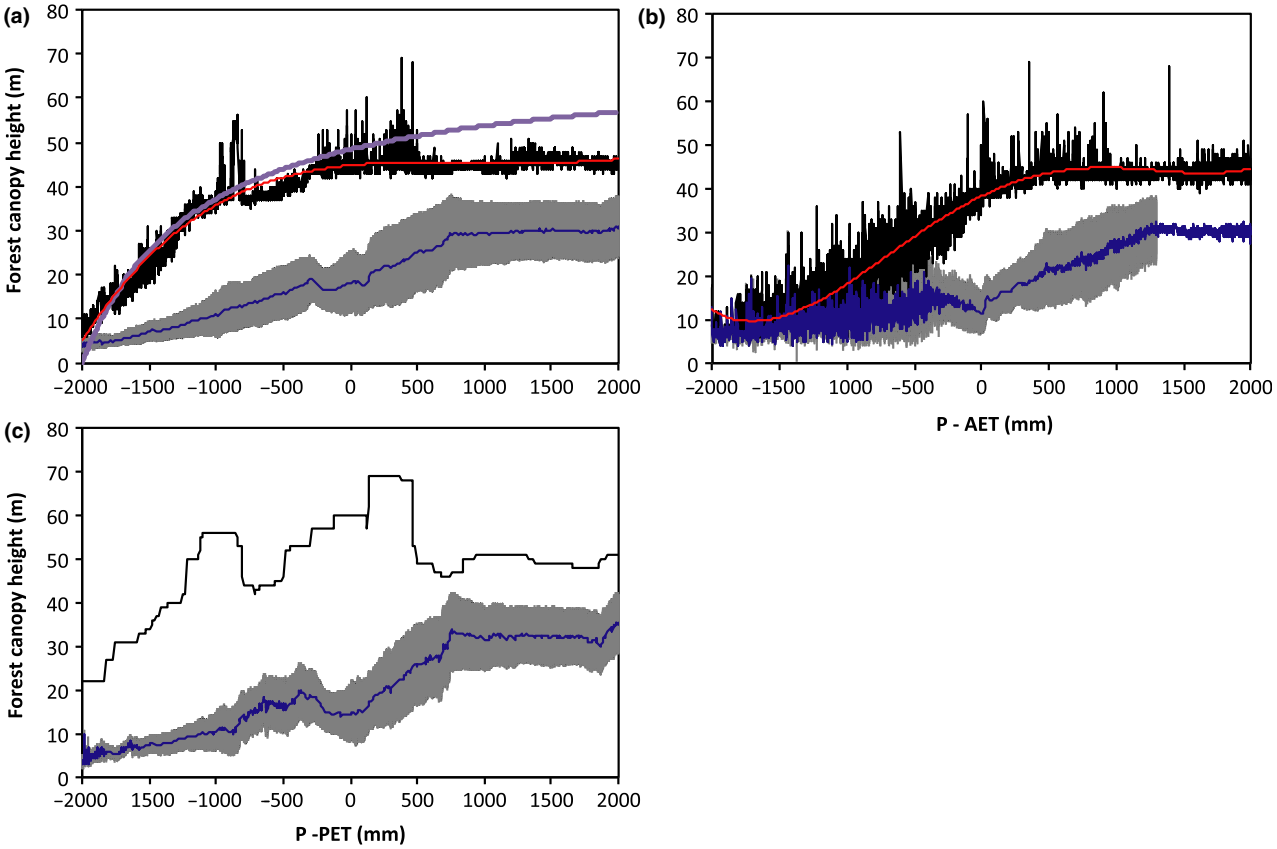

Figure 1 The worldwide maximum (black lines) and mean ± SD (blue lines and grey surface, respectively) observed forest canopy height reached for each value of the difference between precipitation and potential evapotranspiration (P-PET; (a)). The red curve is a polynomial fit of order 4 (adjusted R^2: 0.89; $P < 0.001$; Table 2); The purple curve is a Michaelis–Menten type model $H = H_{max}/((P\text{-}PET)_{Hmax/2} + (P\text{-}PET))$ (R^2: 0.89; $P < 0.001$). (b) Maximum and mean forest height for the difference between precipitation and actual evapotranspiration (P-AET). The red curve is $H_{max} = -1 \times 10^{-12} \times P\text{-}AET^4 - 2 \times 10^{-9} \times P\text{-}AET^3 - 8 \times 10^{-6} \times P\text{-}AET^2 + 1.5 \times 10^{-2} \times P\text{-}AET + 38.3$ (adjusted R^2: 0.92; $P < 0.001$). (c) Maximum forest height yielded by smoothing the maximum height in (a) around the highest value within 250-mm moving windows; Mean forest height yielded by filtering all data to human footprint < 5%.

difference between precipitation (P) and actual evapotranspiration (AET). The global map of yearly actual evapotranspiration from FAO (http://data.fao.org/map?entryId=750d56ca-f92a-405e-8bbc-302221d55917) was used for AET at a 0.0833-degree (5 arc-minutes) spatial resolution for the period 1961–1990. Monthly layers of precipitation were extracted from the CRU CL 2.0 Global Climate Dataset prepared by the Climate Research Unit of the University of East Anglia (http://www.cru.uea.ac.uk/~timm/grid/CRU_CL_2_0.html) to match both the spatial resolution and the reference period.

In our analysis, we preferred the potential evapotranspiration rather than the actual evaporation to also account for the atmospheric evaporative demand and for more homogeneous global coverage. At the leaf scale, this evaporative demand is often measured as vapour pressure deficit (VPD), and, together with stomatal conductance, it controls the rate of transpiration. We therefore checked to what extent changes in PET were proportional to changes in VPD (see below).

Summing monthly P-PET differences on an annual time scale, we also lost information about the seasonal patterns at each site, and specifically the intra-annual temporal distribution of precipitation. For this purpose, a seasonality index (SI) was used (Walsh & Lawler 1981):

$$SI = \frac{1}{P} \times \sum_{1}^{12} \left| MP - \frac{P}{12} \right| \quad (1)$$

where P is the mean annual precipitation and MP is the observed mean monthly precipitation. To test the effects of seasonality and VPD, we took advantage of the BIGFOOT dataset (Turner *et al.* 2012) with micrometeorological measurements from nine flux-tower sites across the Americas. This dataset was disproportionally smaller than our global map, but included contrasting forest types, deciduous and evergreen, from wet and dry biomes, making it a good subset of test conditions for seasonality and VPD effects.

Height growth potential based on P-PET

The three equations (absolute maximum, maximum and mean) were then projected back on the geographical dataset at the global scale to obtain a spatial layer of the potential forest canopy height as a function of P-PET. To test the extent to which height growth potential was realized across all forest stands around the globe, a ratio between the actual observed forest canopy height (H) and the absolute maximum H, maximum H and mean H (eqns 2–4) predicted by the three respective equations was calculated from the spatial layers and represented at the global scale. This ratio, expressed as percentage, is hereafter defined as the per cent of hydrologically predicted height, PHH:

$$PHH_{max*} = H_x / H_{max*}(\text{P-PET}_x) \quad (2)$$

$$PHH_{max} = H_x / H_{max}(\text{P-PET}_x) \quad (3)$$

$$PHH_{mean} = H_x / H_{mean}(\text{P-PET}_x) \quad (4)$$

where H_x is the local forest canopy height at pixel x, and $H_{max*}(\text{P-PET}_x)$, $H_{max}(\text{P-PET}_x)$ and $H_{mean}(\text{P-PET}_x)$ are the derived global absolute maximum, maximum and mean forest canopy height for the P-PET measured at pixel × (from the empiric functions). Values of PHH_{max*} and PHH_{max} theoretically ranged between 0 and 1 (0–100% in graphic presentations), for entirely suppressed H and fully hydrologically predicted H respectively. In contrast, the range of PHH_{mean} inherently included values > 1, for forests exceeding the mean H predicted by their local water availability.

Finally, we assessed the variation of PHH_{max} across latitudinal gradients on six continents, namely North and South America, Europe, Africa, Asia and Australia. For this, we calculated the highest PHH_{max} value reached for each latitudinal increment of 0.25° from 0° to 90°N and 0° to 90°S. Here, we hypothesized that PHH_{max} should decrease when moving poleward because of the increasing importance of temperature over hydrological control.

RESULTS

Forest canopy height and P-PET

There was a quasilinear increase in remotely sensed maximum forest height from 6 m at P-PET = −2000 mm to 40 m at P-PET = −1000 mm (Fig. 1a). The sensitivity of maximum height to P-PET was lower at P-PET greater than −800 mm, stabilizing on 45 m at P-PET > 500 mm. A maximum function $H_{max}(\text{P-PET})$ was empirically constructed from the data in Fig. 1a. This fourth order polynomial function had a highly significant correlation even after adjusting r^2 to the number of observations for each P-PET (eqn 5 in Table 2). A third order polynomial function fitted well too, but eqn 5 was more accurate, and fitted better than a Michaelis–Menten type model. Some observations were above the curve, e.g. up to 56 m and 69 m at P-PET = −850 mm and 380 mm respectively. The first spike can be related to runoff fed tropical forest (e.g. in Bolivia and NW Mexico), whereas the second spike, representing the global maximum, is associated with tropical rain forests in Amazonia and Congo, and coastal forests in higher latitudes (Fig. S1). Notably, the highest canopies (68 and 69 m), were identified in Congo at P-PET of 467 and 381 mm, respectively, whereas the single tallest trees in California and Eastern Australia were not detected (Fig. S2).

The mean forest height increased quasilinearly up to P-PET = 700 mm, where it saturated at 30 m (Fig. 1a). Notably, the linear function $H_{mean} = 19.3 + 0.077*(\text{P-PET})$ was still a valid simplification. A decrease at −400 < P-PET less than −200 mm is explained by the high fraction of temperature limited boreal forest in this water availability range (Fig. S1). Comparing the two curves showed that while the maximum height was sensitive to P-PET mostly at the dry part of the moisture range (P-PET less than −800 mm), the mean height maintained high sensitivity to P-PET across a wider range of forests. The difference between the mean and the maximum curves increased with moisture levels, reaching more than 40 m difference at −800 mm and stabilizing at ca. 20 m difference for P-PET > 500 mm. This suggested that while the variance of height tended to increase with P-PET in dry areas, it was relatively stable, or even decreased, in wet areas. Substituting PET with actual evapotranspiration (AET) produced a relatively similar relationship, albeit with 2–4 fold

Table 2 Equations of forest canopy height as function of P-PET from the global forest dataset correlations in Fig. 1

	Equation	R^2 (adjusted)	P
Eqn 5. Maximum height	$H_{max} = -3.3 \times 10^{-14} \times \text{P-PET}^4 + 6.3 \times 10^{-10} \times \text{P-PET}^3 - 3.9 \times 10^{-6} \times \text{P-PET}^2 + 6.3 \times 10^{-3} \times \text{P-PET} + 44.4$ (5)	0.89	$P < 0.001$
Eqn 6. Absolute maximum height	$H_{max}* = -5.4 \times 10^{-14} \times \text{P-PET}^4 + 9.4 \times 10^{-10} \times \text{P-PET}^3 - 4.9 \times 10^{-6} \times \text{P-PET}^2 + 4.2 \times 10^{-3} \times \text{P-PET} + 58.1$ (6)	0.80	$P < 0.001$
Eqn 7. Mean height	$H_{mean} = 5.8 \times 10^{-14} \times \text{P-PET}^4 + 7.2 \times 10^{-10} \times \text{P-PET}^3 1.3 \times 10^{-6} \times \text{P-PET}^2 + 6.5 \times 10^{-3} \times \text{P-PET} + 20.1$ (7)	0.92	$P < 0.001$

Absolute maximum height was produced by smoothing the observed maximum height around the highest value within P-PET moving windows of 250 mm, to correct for the limited spatial resolution and anthropogenic height suppression.

higher variance in forest height, mostly at P-AET < 0 (Fig. 1b). The increase in maximum forest height with P-AET was more gradual than with P-PET, with maximum heights of 40 m around P-AET = 0, but the mean forest height behaved similarly with both water availability proxies. To reduce the effect of the human footprint on forest height, an absolute maximum curve was created considering only the tallest forests in the analysis (Fig. 1c; termed absolute maximum). Filtering all forest areas for a human footprint < 5% increased the mean forest height by 3–4 m at P-PET > 700 mm (Fig. 1c). The decrease at −400 < P-PET less than −200 mm was more pronounced than in Fig. 1a due to an increase in the relative share of undisturbed, temperature limited and boreal forest (Fig. S1).

Relationship between PET and VPD and the role of precipitation seasonality

Additional water availability parameters were tested on a subset of forest sites offering more detailed information. Monthly mean values of PET and VPD from each of nine examination sites were correlated and yielded linear fits of various slopes and r^2 of 0.55–0.89. Higher monthly PET always meant higher monthly mean VPD at all sites. But overall, at VPD > 1200 Pa, PET seemed to saturate around 150–200 mm month^{-1}, possibly due to stomatal control of water loss in transpiration.

Remotely sensed forest canopy heights of the nine sites correlated well with P-PET (H = 0.05 × P-PET + 15.8; r^2 = 0.92), in agreement with the global trend of mean height (Fig. 1). To test whether tree height decreases with the increase in precipitation seasonality, canopy heights were plotted against the site-specific seasonality index (SI, 0 for equally distributed precipitation amounts across the twelve months of the year), which yielded poor correlation (r^2 = 0.03). For example, trees in the moderately seasonal (0.50 < SI < 0.59) tropical forest in Santarem, Brazil (SI = 0.58, H = 36 m), were considerably taller than trees in the consistently wet (SI = 0.06, H = 23 m) temperate Harvard forest. The height difference was explained by the P-PET in Santarem and Harvard: 366 mm and 208 mm respectively. Likewise, a moderately seasonal temperate forest in western Oregon, USA (SI = 0.53, H = 18 m) was higher than a mildly seasonal (0.40 < SI < 0.49) boreal forest site in Manitoba, Canada (SI = 0.45, H = 12 m). Again, height differences between the two sites were consistent with differences in P-PET: 89 mm and −84 mm in Oregon and Manitoba respectively. Interestingly, among forests of the same biome, height was well correlated with the seasonality index. For example, among temperate forests, there was a trend of decreasing canopy heights between Harvard, Wisconsin and Oregon (23, 19 and 18 m) along an increasing seasonality gradient (SI of 0.06, 0.39 and 0.53).

Height growth potential based on P-PET

The extent to which forest canopies realized their height growth potential as predicted by water availability alone was calculated for all forest sites globally (Fig. 2). The three large tropical forest areas of South America, Central Africa and South-East Asia stood out with absolute maximum height predictability > 50% and maximum height predictability > 60% (Fig. 2a and b). Among these three areas, forests in South-East Asia and specifically in Borneo and New Guinea, made up the largest area where absolute maximum height predictability was > 70%. Temperate forests, mostly in North America, East Asia and along Australia's East coast, also reached canopy heights approaching the maximum height predicted by hydrology. On the contrary, large areas of boreal forest (in North Asia and North America) and sub-tropical forest (mainly in South America and Africa) had maximum height predictability < 40%. The high predictability in wet and tall forests, and low predictability in dry and short forests, indicated the involvement of additional limiting factors (e.g. temperature, radiation, etc.; discussed below), which was probably more pronounced in the drier, shorter and forests. The dichotomy between the two groups of forests (tropical and temperate vs. boreal and sub-tropical) was also observed, albeit with variations, in the mean height predictability map (Fig. 2c). Globally, many canopy heights were at, or above, their hydrologically predicted mean. Yet, some boreal and sub-tropical forests showed mean height predictability < 70%.

Comparing the maps in Fig. 2b and c, forests with low maximum height predictability (PHH_{max} < 40%) had either low mean height predictability (PHH_{mean} < 40%, e.g. in Labrador, Canada; the Kamchatka peninsula in East Siberia;

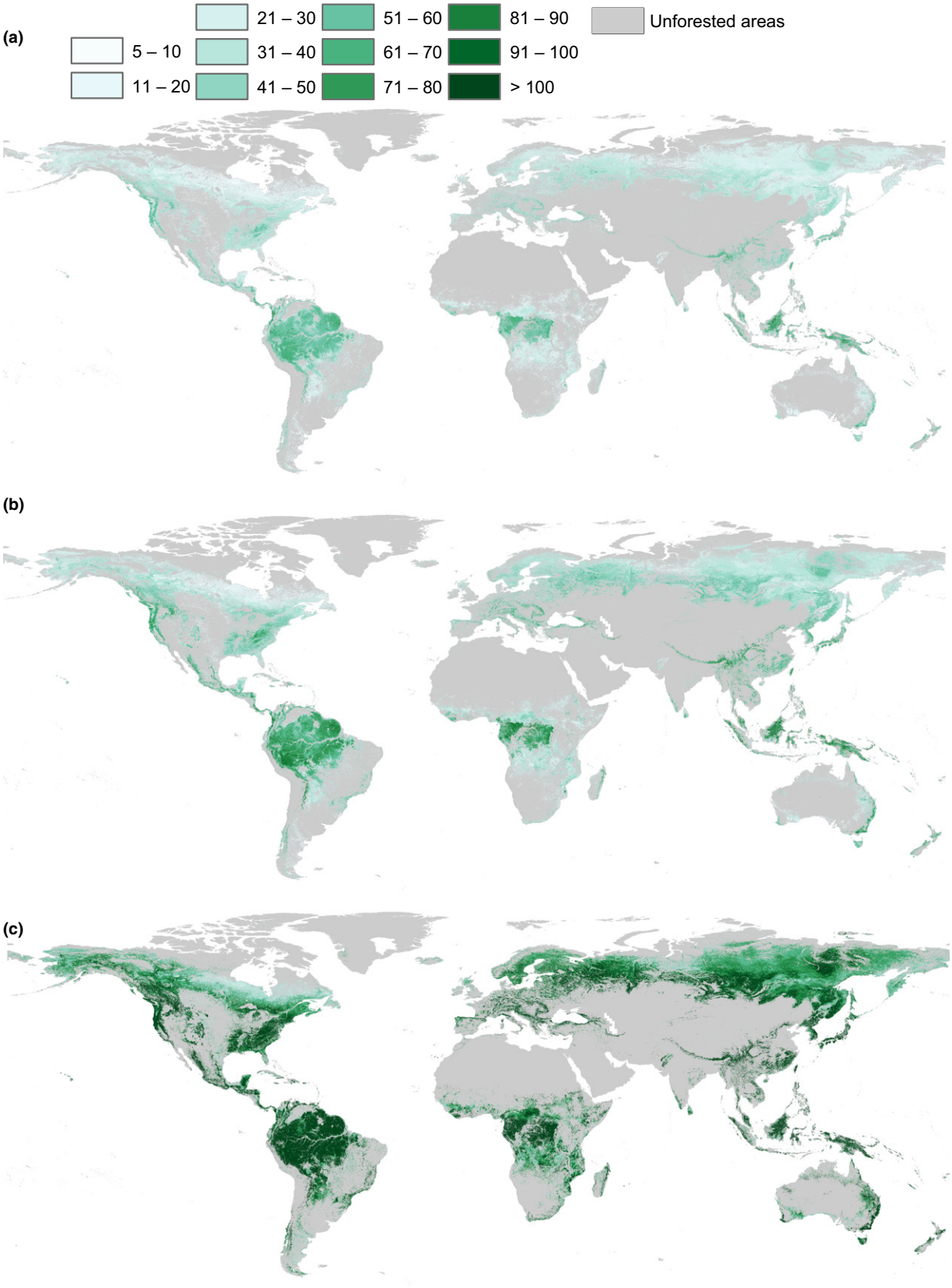

Figure 2 Spatial representation of the Percent of Hydrologically predicted Height (PHH) at the global scale, calculated as the ratio between the locally observed forest canopy height and the absolute maximum (a), maximum (b) and mean (c) forest canopy height for the local P-PET value, based on the equations developed in Fig. 1 (eqns 2–4, see text). PHH indicates the extent to which actual forest canopies realized their height growth potential as predicted by water availability alone (WGS 84; 0.0083 degree).

and Scotland's highlands) or high mean height predictability (PHH_{mean} > 70%, e.g. in Bolivia; the Yucatan peninsula; NW Mexico; Ethiopia's highlands; and the Baikal region in Siberia). Evidently, while the first group was characterized by short canopies in wet areas (unexpectedly low H at high P-PET, partly explained by mean wind speed > 8 m s^{-1} in those areas), the second group was characterized by tall canopies in dry areas (unexpectedly high H at low P-PET, hinting to localized inflows of water from neighbouring regions). Such pattern was not observed at the high end of PHH values, as all forests with high maximum height predictability (PHH_{max} > 60%) had high predictability of mean height (PHH_{mean} > 100%). A global trend towards lower maximum height predictability at high latitudes was observed across all continents, in both northern and southern hemispheres (Fig. 3). The decline typically started around the edges of the tropics (23.5°N and 23.5°S), where PHH_{max} > 80%, and continued monotonically towards the northern and southern timberlines. Zooming in on specific geographical areas with steep PHH_{max} gradients seemed to demonstrate the effect of anthropogenic disturbance (Fig. 4). Relying on the robust relationships between forest height and water availability, unexpected local decreases in PHH were observed in suppressed forests close to populated areas, compared to nearby protected or secluded areas, where forests approached their full height potential.

DISCUSSION

The global analysis presented in this study provides quantitative evidence for the control of water availability over forest canopy height around the world. Although the relationships between water availability and tree height have been assessed locally in numerous studies (Williams *et al.* 1996; Eamus *et al.* 2000; Albaugh *et al.* 2004; Koch *et al.* 2004; Givnish *et al.* 2014), to the best of our knowledge we conducted here the first global analysis. In forest research, maximum tree height has been identified as indicator of 'site quality' for even-aged forest stands (Burkhart & Tome 2012). Strong relationships between site conditions, maximum tree height and the productive potential of stands exist (McDill & Amateis 1992; Burkhart & Tome 2012), but are complicated by an age-related growth decline (Robichaud & Methven 1993). The observed significant and positive correlations between forest height and P-PET (Fig. 1) support the role of hydraulic limitation on tree height (Friend 1993) i.e. that water availability exerts a direct limitation on the maximum height trees can assume (Sala & Hoch 2009). In turn, the mechanistic association between tree height and water availability (Ryan & Yoder 1997; Koch *et al.* 2004; Niklas & Spatz 2004; Ryan *et al.* 2006; Domec *et al.* 2008) is essential for attributing causality to the correlations we presented. Our results further complement the well known hydraulic limitation on tree height, by: (1) showing that the mean, and not only the maximum, canopy height also depends on moisture conditions; and (2) providing evidence for the dominance of water limitations over other limiting factors controlling tree height. The second point rests on the fact that, using the observed relationships between mean height and P-PET (eqn 7), we were able to reproduce the height of forest canopies around the globe (green shades in Fig. 2c). Substituting PET with AET yielded a similar correlation with forest canopy height, further supporting our results. The higher variance in maximum forest height at P-AET < 0 (Fig. 1b) can be related to variations

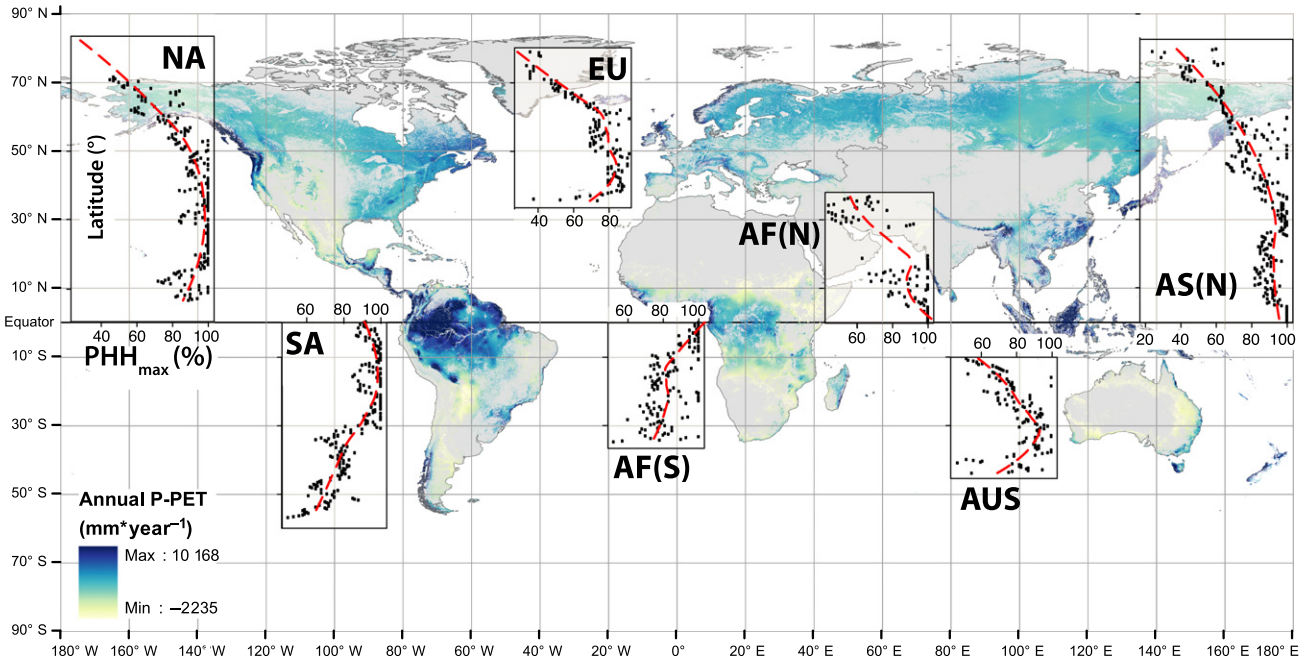

Figure 3 Latitudinal trends in the predictability of maximum forest height based on water availability (PHH_{max}, %) across northern (N) and southern (S) hemisphere sections of the six continents, overlaid on the global map of P-PET. Data points in the graphs are the maximum PHH_{max} (%) for each latitude and continent; red curves have been adjusted with a loess function to show the latitudinal trend. NA, North America; SA, South America; EU, Europe; AF, Africa; AS, Asia; AUS, Australia (WGS 84; 0.0083 degree).

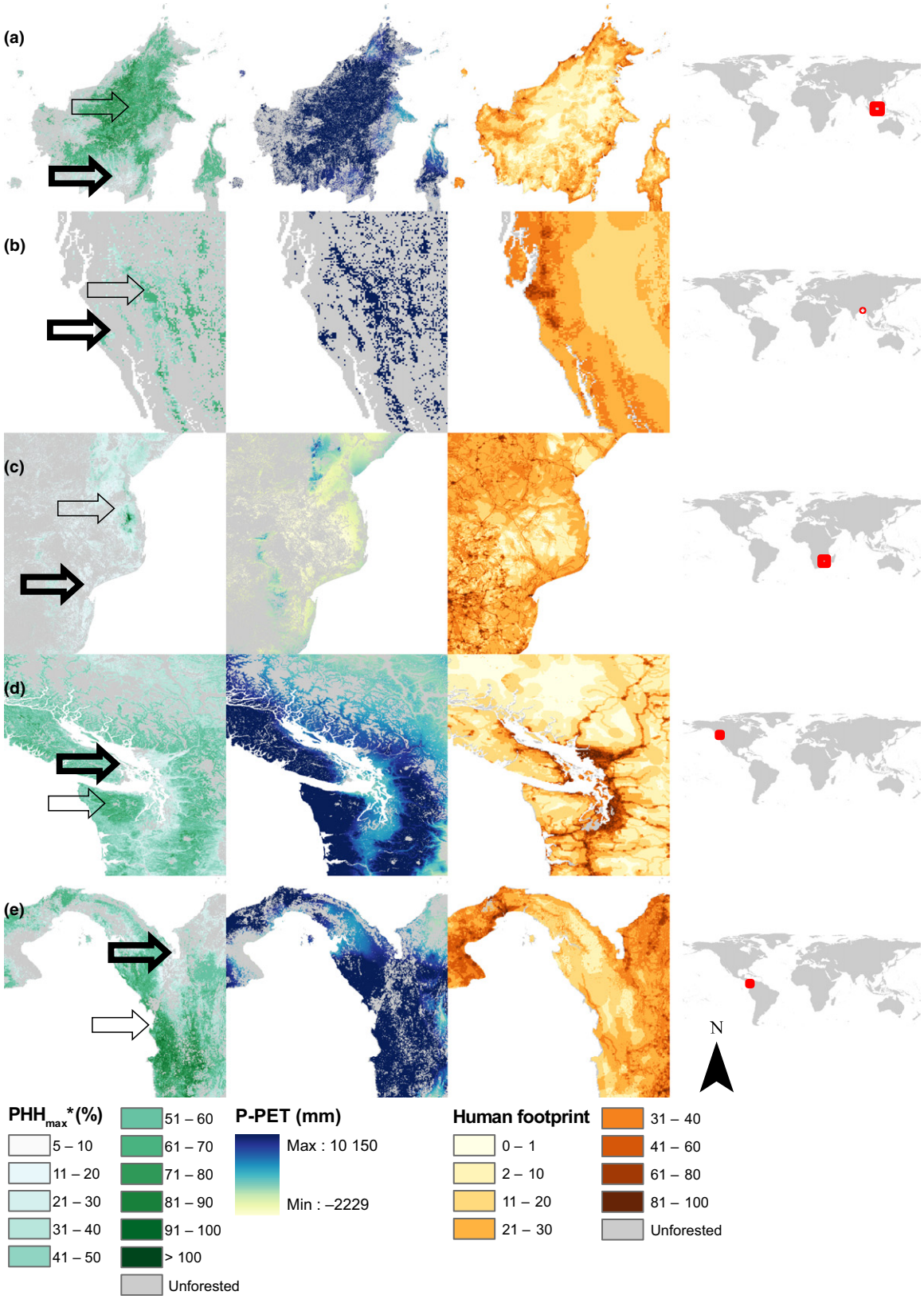

Figure 4 Five examples of human-induced forest decline from around the globe: Borneo (a); Myanmar (b); Mozambique (c); Vancouver, Canada (d) and Columbia-Panama border region (e). Each example shows a gradient in maximum forest height predictability (PHH_{max}; left column) from canopies close to the maximum height permitted by their local water availability ($PHH_{max} > 60\%$, open arrows) to suppressed canopies ($PHH_{max} < 40\%$, open-bold arrows). These suppressed canopies are at similar P-PET (middle panels) as the tall canopies, but at dramatically higher human footprint index (right panels) (WGS 84; 0.0083 degree).

in evapotranspiration and the level of canopy conductance to water vapour (e.g. via stomatal control of water loss in transpiration and via boundary layer effects) compared to the physical nature of PET. Such variations are expected more in dry than in wet sites. The higher sensitivity to P-PET of H_{mean} than H_{max} in wet areas might be related to their higher biodiversity compared with drier areas (Gaston 2000) i.e. that in wet forests many species grow taller, whereas in dry forests specialization or local adaptation may give advantage to only a few species.

The PET term was important to capture the atmospheric evaporative demand. If tree height is limited hydraulically, then water potential must be sensed in terminal shoots, where it is co-governed by the vapour pressure deficit, VPD. The good correlation between PET and VPD, though not surprising, supports the use of P-PET as integrator of the water balance in soil, and the evaporative demand that acts on leaves. However, using annual P-PET as a proxy for water availability is not without its limitations. The world's tallest trees thrive only in consistently humid sites (*Sequoia sempervirens* in California, USA and *Eucalyptus regnans* in Victoria, Australia), while other wet sites with high P-PET can have dry periods. Due to the limited spatial resolution, individual trees of > 70 m height escaped the satellite observation. Seasonality explained observed height differences among sites within the same biome, but not across different biomes and large P-PET differences. Hence, seasonality effects are probably overridden by the larger differences in the annual water balance, and are therefore less important at the global scale (Moles *et al*. 2009). In addition, trees, having higher rooting depth than shrubs and non-woody plants (Canadell *et al*. 1996) can also buffer seasonality effects and thus integrate moisture signatures over longer periods (Sarris *et al*. 2007).

Inconsistencies between forest height and P-PET were not uncommon in our global analysis. Areas with low values of predictability (Figs. 2–4) have a relatively low degree of association between height and P-PET, and therefore indicate an increasing role of other growth limitations. These limitations can be roughly divided into five categories: (1) Environmental limitations, such as by low nutrients or temperature, maximum wind speed and biotic factors (e.g. inter- and intraspecific competition and pathogens); (2) Genetic limitations, such as tree species and provenances (setting height growth potential) and tree age; (3) Interactions between environmental and genetic limitations, i.e. the ability of a certain tree species to occupy a specific site, i.e. the ecological niche; (4) The occurrence of natural disturbance, e.g. wildfire, climate extreme, insect outbreak, etc. and (v) Anthropogenic disturbance, either directly through logging, or indirectly through climate change. Strong latitudinal trends of maximum height predictability across all continents (Fig. 3) extend on the observation of a sharp decrease in the height of herbs and shrubs at the edge of the tropics (Moles *et al*. 2009) and indicate the limiting role of temperature. Low temperature limits tree growth even at low latitudes, i.e. with elevation. The montane thermal belt covers 5.29% of the global terrestrial area outside Antarctica (Körner *et al*. 2011). Assuming half of it as forested, and considering the global forest area fraction (Table S1), 8.65% of the world forests are montane and hence might be of lower height than predicted by hydrology alone. Evidence for the role of anthropogenic disturbance comes from comparing the extent of height predictability in the temperate forests (40°N–60°N) east and west from the North Atlantic. The suppressed forests of Europe reached 80% of their maximum height (predicted by P-PET), while North-American forests started at 95% in 40°N, gradually decreasing to 80% at 60°N (Fig. 3). Similarly, the absolute maximum function (eqn 6) peaked at 57 m, much above the H_{max} function peak at 45 m. Our local examples from a variety of forest biomes (Fig. 4) further highlight the negative impact of human footprint on actual forest heights relative to their potential. This effect was more pronounced in wet sites, since considering only less-disturbed forests increased the mean forest height mostly at P-PET > 700 mm (Fig. 1c).

The combination of a strong association between forest height and P-PET (Fig. 1), and the degree to which hydrology can explain observed variations in height (Fig. 2) makes an appealing case for their application in various modelling purposes. For example, our results can be useful for: (1) predictions of forest distribution and changes in biomass under climate change scenarios, e.g. by creating a climate change scenario-driven global P-PET map, which, in turn, can be used to predict canopy height distribution; (2) reconstructions of past forest dynamics using available estimates of past climatic conditions; (3) studying the impact of anthropogenic disturbance on height, e.g. using case studies in forests that are highly controlled by water availability and (4) quantifying the anthropogenic control over tree turnover (harvest cycles) from differences between potential and actual forest heights.

ACKNOWLEDGEMENTS

The authors thank Yann Vitasse, Günter Hoch and Raphael Weber of the University of Basel and three anonymous reviewers for their useful comments on an earlier version of this paper. Josh Fisher and Marc Simard of NASA Jet Propulsion Laboratory and David Turner of Oregon State University are acknowledged for permissions for using their respective databases. TK was funded by the Swiss National Science Foundation project FORCARB (31003A_14753/1) allocated to CK and by the Plant Fellows program of the Zürich-Basel Plant Science Center (PSC) through the EU FP7 Marie Curie action. CR received funding from European Research Council (ERC) grant no. 2333 (project TREELIM to CK) during parts of the work for this study.

AUTHORSHIP

TK designed the study; CR performed the mapping and most correlations; TK, CR and CK contributed to the analysis and wrote the paper.

REFERENCES

Albaugh, T.J., Lee Allen, H., Dougherty, P.M. & Johnsen, K.H. (2004). Long term growth responses of loblolly pine to optimal nutrient and water resource availability. *Forest Ecol. Manage*., 192, 3–19.

Arino, O., Bicheron, P., Achard, F., Latham, J., Witt, R. & Weber, J.-L. (2008). GlobeCover, the most detailed portrait of Earth. *ESA Bull.*, 136, 24–31.

Burkhart, H.E. & Tome, M. (2012). Evaluating site quality. *Modeling Forest Trees and Stands*. Springer, Netherlands, pp. 131–173.

Canadell, J., Jackson, R.B., Ehleringer, J.R., Mooney, H.A., Sala, O.E. & Schulze, E.D. (1996). Maximum rooting depth of vegetation types at the global scale. *Oecologia*, 108, 583–595.

Choi, S., Ni, X., Shi, Y., Ganguly, S., Zhang, G., Duong, H.V. *et al.* (2013). Allometric scaling and resource limitations model of tree heights: part 2. Site based testing of the model. *Remote Sens.*, 5, 202–223.

Domec, J.C., Lachenbruch, B., Meinzer, F.C., Woodruff, D.R., Warren, J.M. & McCulloh, K.A. (2008). Maximum height in a conifer is associated with conflicting requirements for xylem design. *Proc. Natl Acad. Sci. USA*, 105, 12069–12074.

Eamus, D., O'Grady, A.P. & Hutley, L. (2000). Dry season conditions determine wet season water use in the wet–tropical savannas of northern Australia. *Tree Physiol.*, 20, 1219–1226.

Friend, A.D. (1993). The prediction and physiological significance of tree height. In: *Vegetation Dynamics and Global Change* (eds Solomon, A.M., Shugart, H.H.). Chapman & Hall, New York, pp. 101–115.

Gaston, K.J. (2000). Global patterns in biodiversity. *Nature*, 405, 220–227.

Givnish, T.J., Wong, S.C., Stuart-Williams, H., Holloway-Phillips, M. & Farquhar, G.D. (2014) Determinants of maximum tree height in *Eucalyptus* species along a rainfall gradient in Victoria, Australia. *Ecology*, 95, 2991–3007.

Hijmans, R.J., Cameron, S.E., Parra, J.L., Jones, P.J. & Jarvis, A. (2005). Very high resolution interpolated climate surfaces for global land areas. *Intl. J. Climatol.*, 25, 1965–1978.

Koch, G.W., Sillett, S.C., Jennings, G.M. & Davis, S.D. (2004). The limits to tree height. *Nature*, 428, 851–854.

Körner, C., Paulsen, J. & Spehn, E.M. (2011). A definition of mountains and their bioclimatic belts for global comparisons of biodiversity data. *Alp. Botany*, 121, 73–78.

Lefsky, M.A.A. (2010) A global forest canopy height map from the Moderate Resolution Imaging Spectroradiometer and the Geoscience Laser Altimeter System. *Geophys. Res. Let.* 37, L15401.

McDill, M.E. & Amateis, R.L. (1992). Measuring forest site quality using the parameters of a dimensionally compatible height growth function. *Forest Sci.*, 38, 409–429.

Moles, A.T., Warton, D.I., Warman, L., Swenson, N.G., Laffan, S.W., Zanne, A.E. *et al.* (2009). Global patterns in plant height. *J. Ecol.*, 97, 923–932.

Niklas, K.J. & Spatz, H.C. (2004). Growth and hydraulic (not mechanical) constraints govern the scaling of tree height and mass. *Proc. Natl Acad. Sci. USA*, 101, 15661–15663.

Pennisi, E. (2005). The sky is not the limit. *Science*, 310, 1896–1897.

Piedallu, C., Gégout, J.C., Perez, V. & Lebourgeois, F. (2013). (2013) Soil water balance performs better than climatic water variables in tree species distribution modelling. *Glob. Ecology Biogeog.*, 22, 470–482.

R Development Core Team (2011). R: a language and environment for statistical computing. R Foundation for Statistical Computing, Vienna

Robichaud, E. & Methven, I.R. (1993). The effect of site quality on the timing of stand breakup, tree longevity, and the maximum attainable height of black spruce. *Canadian J. Forest Res.*, 23, 1514–1519.

Ryan, M.G. & Yoder, B.J. (1997) Hydraulic limits to tree height and tree growth. *Biosci.* 47, 235–242.

Ryan, M.G., Phillips, N. & Bond, B.J. (2006). The hydraulic limitation hypothesis revisited. *Plant, Cell Environ.*, 29, 367–381.

Sala, A. & Hoch, G. (2009). Height-related growth declines in ponderosa pine are not due to carbon limitation. *Plant, Cell Environ.*, 32, 22–30.

Sanderson, E.W., Jaiteh, M., Levy, M.A., Redford, K.H., Wannebo, A.V. & Woolmer, G. (2002). The Human Footprint and the Last of the Wild: the human footprint is a global map of human influence on the land surface, which suggests that human beings are stewards of nature, whether we like it or not. *Bioscience*, 52, 891–904.

Sarris, D., Christodoulakis, D. & Körner, C. (2007). Recent decline in precipitation and tree growth in the eastern Mediterranean. *Glob. Change Biol.*, 13, 1187–1200.

Shi, Y., Choi, S., Ni, X., Ganguly, S., Zhang, G., Duong, H.V. *et al.* (2013). Allometric scaling and resource limitations model of tree heights: part 1. Model optimization and testing over continental USA. *Remote Sens.*, 5, 284–306.

Simard, M., Pinto, N., Fisher, J.B. & Baccini, A. (2011). Mapping forest canopy height globally with spaceborne lidar. *J. Geophys. Res. Biogeosciences*, 116(G4), G04021.

Toniato, M.T.Z. & de Oliveira-Filho, A.T. (2004). Variations in tree community composition and structure in a fragment of tropical semideciduous forest in southeastern Brazil related to different human disturbance histories. *Forest Ecol. Manage.*, 198, 319–339.

Trabucco, A. & Zomer, R.J. (2010) Global soil water balance geospatial database. CGIAR Consortium for Spatial Information. Published online, available from the CGIAR-CSI GeoPortal at: http://www.cgiar-csi. org.

Turner, D.P., Gregory, M.J. & Ritts, W.D. (2012) BIGFOOT Meteorological Data for North and South American Sites, 1991-2004. Data set. Available on-line (http://daac.ornl.gov/) from Oak Ridge National Laboratory Distributed Active Archive Center, Oak Ridge, Tennessee, USA. Available at: http://dx.doi.org/10.3334/ORNLDAAC/1065. Diurnal means of vapor pressure deficit for North and Soutn American sites.

Walsh, R.P.D. & Lawler, D.M. (1981). Rainfall seasonality: description, spatial patterns and change through time. *Weather*, 36, 201–208.

Williams, R.J., Duff, G.A., Bowman, D.M.J. & Cook, G.D. (1996). Variation in the composition and structure of tropical savannas as a function of rainfall and soil texture along a large-scale climatic gradient in the Northern Territory. *Australia. J. Biogeog.*, 23, 747–756.

Xu, C.Y. & Singh, V.P. (2002). Cross comparison of empirical equations for calculating potential evapotranspiration with data from Switzerland. *Water Resources Manage.*, 16, 197–219.

Zomer, R.J., Trabucco, A., vanStrassen, O. & Bossio, D.A. (2006) Carbon, land and water: a global analysis of the hydrologic dimensions of climate change mitigation through afforestation/reforestation. Research Report 101, International Water Management Institute.

Zomer, R.J., Trabucco, A., Bossio, D.A. & Verchot, L.V. (2008). Climate change mitigation: a spatial analysis of global land suitability for clean development mechanism afforestation and reforestation. *Agric. Ecosys. Environ.*, 126, 67–80.

SUPPORTING INFORMATION

Additional Supporting Information may be downloaded via the online version of this article at Wiley Online Library (www.ecologyletters.com).

Editor, Arne Mooers
Manuscript received 18 June 2015
First decision made 26 July 2015
Second decision made 13 August 2015
Manuscript accepted 24 August 2015